HHS Public Access

Author manuscript

Analyst. Author manuscript; available in PMC 2017 February 21.

Published in final edited form as:

Analyst. 2016 February 21; 141(4): 1519–1529. doi:10.1039/c5an02220g.

2,4-Toluene Diisocyanate Detection in Liquid and Gas Environments through Electrochemical Oxidation in an Ionic Liquid

Lu Lin, **Abdul Rehman**, **Xiaowei Chi**, and **Xiangqun Zeng***

Department of Chemistry, Oakland University, Rochester, MI 48309, USA

Abstract

The electrochemical oxidation of 2,4-toluene diisocyanate (2,4-TDI) in an ionic liquid (IL) has been systematically characterized to determine plausible electrochemical and chemical reaction mechanisms and to define the optimal detection methods for such a highly significant analyte. It has been found that the use of an IL as the electrolyte allows the oxidation of 2,4-TDI to occur at a less positive anodic potential with no side reactions as compared to traditional acetonitrile based electrolytes. UV-Vis, FT-IR, Cyclic Voltammetry and Electrochemical Impedance Spectroscopy (EIS) studies have revealed the unique mechanisms of dimerization of 2,4-TDI at the electrode interface by self-addition reactions, which can be utilized to improve the selectivity of detection. The study of 2,4-TDI redox chemistry further facilitates the development of a robust amperometric sensing methodology by selecting a hydrophobic IL ($[C_4mpy][NTf_2]$) and by restricting the potential window to only include the oxidation process. Thus, this innovative electrochemical sensor is capable of avoiding the two most ubiquitous interferents in ambient conditions (i.e. humidity and oxygen), thereby enhancing the sensor performance and reliability for real world applications. The method was established to detect 2,4–TDI in both liquid and gas phases. The limits of detection (LOD) values were 130.2 ppm and 0.7862 ppm, respectively, for the two phases, and are comparable to the safety standards reported by NIOSH. The as-developed 2.4-TDI amperometric sensor exhibits a sensitivity of 1.939 μA/ppm. Moreover, due to the simplicity of design and the use of an IL both as a solvent and non-volatile electrolyte, the sensor has the potential to be miniaturized for smart sensing protocols in distributed sensor applications.

INTRODUCTION

Recent explosions in Tianjin, the port city of China wherein chemicals, such as toluene diisocyanates (2,4-TDI) and calcium carbide, have been stored, thereby killing more than 50 people and leaving several hundred injured, has reemphasized the need for detection of these compounds in liquid and gas phases with minimum human intervention.[1] As reported, diisocyanates[2] are low molecular weight significantly toxic compounds that violently react

***Corresponding Author (zeng@oakland.edu)**.

A. Rehman is currently working at: Department of Chemistry, King Fahd University of Petroleum and Minerals (KFUPM), Dhahran 31261, Kingdom of Saudi Arabia (KSA)

Supplementary Information: Schemes S1-S2, Figures S1-S5, and Table S1-S2 as noted in the text is provided in supplementary information and is available free of charge via http://pubs.rsc.org

with water and other chemicals to cause explosions; however, they are highly valuable in the manufacturing industry of polyurethane-based products such as foams, elastomers and coatings. These products are used everywhere in people's daily life because of their durability against chemical damage, colorfastness, and abrasive resistance. However, their manufacturing and product degradation processes cause the diisocyanates to be airborne, thereby posing an adverse challenge for environmental protection and occupational health.[3, 4] In addition, their short-term exposure can cause allergic sensitization, severe irritation of the skin and eyes, as well as problems in respiratory, gastrointestinal and even central nervous systems, whereas long-term exposure can affect lung function.[5] Results from animal studies have also reported a significant increase of tumor cells in organs, such as the pancreas, liver and mammary glands, after exposure to diisocyanates.[6] Therefore, diisocyanates have been classified in Group 2B (possible human carcinogen) by the International Agency for Research on Cancer (IARC).

To avoid these adverse health, environmental, and even life safety threats, accurate and fast diisocyanate detection in real world environments is extremely significant. Both instrumental and continuous monitoring methods have been developed in this regard as reviewed by Guglya.[2] As shown in Table S1, for the instrumental methods,[7] such as high performance liquid chromatography (HPLC),[8, 9] capillary gas chromatography (CGC) with flame ionization[10, 11] and ion chromatography with UV detection,[12, 13] the derivatization and extraction steps are quite time-consuming. Moreover, such offline strategies provide significant statistical differences as compared to online protocols.[14] On the other hand, the most conventional colorimetric method[15] has interference problems, especially from humidity in the air. Infrared spectrophotometric methods[16] based on quantitative measurements of C-H deformation vibration at the aromatic ring has also been reported; however, it requires large sampling amounts and multiple steps of sample preparation. Biological monitoring including the measurement of diisocyanate specific antibodies in serum, diisocyanate derived biomarkers in blood and urine and ELISA based methods have also been studied,[17] but these methods lack the specificity for different diisocyanates while specialized instrumentation is a requirement. Smart sensors can be an efficient substitution in such a situation, which can continuously monitor these hazardous compounds in actual workplace conditions. Morrison et al. made the first attempt in this regard using coated piezoelectric crystals.[18] However, the universal sensitivity of the technique makes it unsuitable for measurement, especially in humid environments. Electrochemical sensors have historically proven to be an ideal detection platform due to its simplicity in design, direct transduction signal readout, fast response times, good selectivities and sensitivities.[19-21,22,23] Electrochemical sensors require the use of an electrolyte; diisocyanates are not stable in many conventional electrolytes, especially aqueous electrolytes, limiting the development of such electrochemical sensors.

Ionic liquids (ILs), on the contrary, have such unique features[24] that resist against chemical interferences and facilitate new electrochemical reactions to occur that would otherwise not be feasible in traditional aqueous or non-aqueous electrolytes. The benefits of ILs for electrochemistry has been summarized in the study by Liu et al[25] on the interface chemistry of IL/electrode. Our group has been utilizing the benefits of ILs in developing gas sensors over past ten years.[26-31] In many gas sensor applications, the presence of oxygen, being

ubiquitous in nature, interferes strongly with electrochemical processes by forming superoxide radicals and thus complicates sensor performance. The superoxide radical has been reported to be relatively stable in ILs and is positively utilized for mechanism explorations and sensing enhancements.[27, 32, 33] However, if such reactions can be avoided, it could simplify sensor developments. In the current study, we developed a simple electrochemical method for direct, qualitative and quantitative isocyanates detection with the capability for future sensor miniaturization. As one of the most common airborne isocyanates, 2,4-TDI was selected as a representative analyte for this study. Isocyanates react with water, alcohols, acids, and organic solvents that have primary or secondary amine functional groups.[34] The extent of their reactivity depends on the activity of hydrogen species in the solvent compounds, steric hindrance, basicity and the electronegativity of the substituent side groups of the solvent molecules. Therefore, non-aqueous solvent systems without a primary or secondary amine, but with lower basicity and larger electronegativity branch chains, are preferred for isocyanate detection. Based on this, the ionic liquid $[C_4mpy][NTf_2]$ was chosen as the solvent as well as the supporting electrolyte because the pyrrolidinium cation is relatively chemically inert and all C-H bonds in the $[C_4mpy]^+$ cation structure are saturated. Moreover, $[NTf_2]^-$ based ILs with conjugated structures exhibit better electrochemical stability than others, such as $[BF_4]^-$ and $[PF_6]^-$, based systems.[27] We first investigated the redox processes of 2,4-TDI in ILs as well as its redox mechanism at the electrochemical interface. Based on the knowledge gained in this mechanistic study, we developed a new electrochemical methodology for the detection of 2,4-TDI in the liquid phase as well as the gas phase. The analytical performance of the so presented electrochemical ionic liquid sensor meets the safety standards of National agencies and thus this sensor is envisioned to be competitive compared to current commercially available technologies for diisocyanate detection.

EXPERIMENTAL SECTION

Chemicals

2,4-toluene diisocyanate (2,4-TDI) (**Scheme S1A**) was purchased from *Fluka* with 99.9% purity. 1-Butyl-1-methylpyrrolidinium bis(trifluoromethylsulfonyl) imide, abbreviated as $[C_4mpy][NTf_2]$ or $[Bmpy][NTf_2]$ (**Scheme S1B**), was purchased from *Ionic Liquids Technologies Inc.* with 99% purity and was stored in a vacuum dry chamber (*Shel Lab* model no. 1415M) under room temperature and a vacuum pressure up to 18 inch Hg. Tetrabutylammonium perchlorate (TBAP) was purchased from *Fluka* at assay grade (≥99.0%). Prior to the measurements, IL aliquots were purged with N_2 (*Airgas* compressed nitrogen) for 12 hours to exclude O_2 and moisture as well as to maintain the same electrolyte condition. Dry air (*Airgas*, breathing grade) was utilized as the background gas for most characterization tests.

Electrodes

A planar glassy carbon electrode (purchased from *CH Instruments, Inc.*) was used as the working electrode. The geometric surface area was 0.0707 cm^2. The reference and counter electrodes were silver wire and platinum wire, respectively. The diameters for both these electrodes were 0.5 mm. The working electrode was first polished using *Buehler*

micropolish 1.0 micron alpha alumina-water slurry followed by 0.05 micron gamma alumina-water slurry, then sonicated using a *Branson* 3510 ultrasonic unit with deionized water for 10 minutes. In the final step, the electrode was rinsed with deionized water and dried with N_2 immediately. To eliminate the influence from potential drifts of the silver quasi-reference electrode, we used the Fc/Fc^+ redox couple to calibrate the potentials. For gas phase detection, the carbon electrode was prepared by loading a graphite ink onto a Teflon membrane (*Interstate*, PM71W). The ink[36] consists of 40.62 mg graphite (*Aldrich*, < 20 μm, synthetic), 768 μL water, 200 μL ethanol and 32 μL 5 wt% Nafion water dispersion (*Aldrich*). The loading amount is 10.35 mg/cm^2.

Electrochemical Cell

A conventional three electrode cell was employed in this study. The electrodes were fixed via Teflon tape and housed in a glass tube, a cross section of which is shown in **Scheme S1C**. The bottom part of this cell was immersed in a silica oil bath set at room temperature (25 °C). Pure N_2 flew into the electrochemical cell via *Tygon* PVC gas tubing (ϕ = 1 mm). The gas was then left to diffuse through the IL until the gas pressure reached an equilibration state between the gas and liquid phases prior to the measurements. This typically takes about 30 minutes. The gas outlet was connected to the vacuum vent to avoid buildup of gas in the electrochemical cell.

Electrochemical Experiments

The *Gamry* 4-channel workstation was used to perform CV, EIS and Chronoamperometry measurements of the 2,4-TDI redox processes. For EIS measurements, a 5 mV AC voltage was applied under open circuit conditions. Initial experiments involved adding 2,4-TDI to the ionic liquid, mixing, and degassing by N_2 before each measurement. Chronoamperometry measurements were performed for detection of gas phase 2,4-TDI. Because 2,4-TDI has a vapor pressure of 0.05 mmHg at 25 °C,[35] gas phase 2,4-TDI was generated by bubbling air through 2,4-TDI liquid. It was subsequently diluted with another air flow gas via two *Tygon* PVC gas tubings (ϕ = 1 mm), one of which was the pure air gas channel (path 1) and the other was the channel (path 2) to bring out the gas phase 2,4-TDI by flowing air. A cross-section of this sampling system is depicted in **Scheme S2**. Total gas flow rate was maintained at 200 sccm. Concentrations of gas phase 2,4-TDI were prepared by increasing the flowrate of path 2 from 0 to 100 sccm, with 20 sccm per increment. Such a gas sensor testing system has been described in detail elsewhere.[36] The detailed calculation of TDI concentration by this flow system is elaborated upon in the supplementary information.

RESULTS AND DISCUSSION

Characterization of 2,4-TDI Redox Processes

Effects of the Supporting Electrolyte and Environmental Conditions—Ionic liquids (ILs) have been shown to have a significant effect on the redox behavior of organic compounds. These effects can be the shifting of oxidation and/or reduction potentials, stabilizing the redox reaction products, inducing certain additional chemical reactions, or even changes in the electrochemical reaction mechanism (e.g. the two one-electron reduction

waves of dinitrobenzene in acetonitrile is reportedly collapsed to a single two-electron wave in ILs such as [C_4mim][BF_4]).[37] Such anomalies due to the presence of IL electrolytes are usually ascribed to the strong ion-pairing in ILs. In a series of computational studies, Fry et al.[38] have examined and reported the interactions between solvent, electrolytic ions, and electroactive species, indicating that the redox potentials can be lowered when ion-pairing with the electrolyte was included. We hypothesize that similar shifts in the oxidation mechanisms of the analytes (i.e. 2,4-TDI) can have significant implications on the development of a more efficient isocyanate electrochemical sensor. Therefore, cyclic voltammetry (CV) was first utilized to characterize an isocyanate redox activity in two non-aqueous solvents (i.e. acetonitrile and IL [C_4mpy][NTf_2]). **Figure 1A** presents the cyclic voltammogram of 2,4-TDI in both solvents, whereas nitrogen was used as the background. In the case of acetonitrile, the oxidation of 2,4-TDI occurred at 1.96 V. On the other hand, there was no redox peak observed in the pure IL indicating that the electrochemical system comprising IL is stable in this potential region. In the presenece of 2,4-TDI in the IL, the electrochemical oxidation peak of 2,4-TDI was observed at a less positive anodic potential (1.38 V) than in acetonitrile (1.96 V). Moreover, though the oxidation peak currents have similar values in both electrolytes, multiple shoulder peaks and a broad small reduction peak were observed before the major oxidation peak in the acetonitrile system, suggesting that the 2,4-TDI oxidation process in acetonitrile involves multiple steps. Such complicated redox mechanisms usually cause difficulty in quantitative analysis due to poor reproducibility and are not desirable for electroanalytical method development. In contrast, in the [C_4mpy][NTf_2] system, it showed one single and clear oxidation peak, which can be used for analytical quantification. Thus, utilization of [C_4mpy][NTf_2] was validated to be suitable for electrochemical detection of 2,4-TDI, as has been done by our group for various different analyte targets.[28, 30, 31, 33, 39] In [C_4mpy][NTf_2], the oxidation peak current of 2,4-TDI was approximately seven times larger than that of the reduction peak, as shown in **Figure 1A**. Therefore, it is also clear that the oxidation process is capable of providing better sensitivity for the detection of 2,4-TDI (**Figure 1B**) and can be used for further quantifications. It was also found that the reduction process would interfere with the current signals of the oxidation process as well. As shown in **Figure 1A**, when the reduction process occurred first, the 2,4-TDI concentration would decrease in the region near the electrode surface leading to a decreased TDI oxidation signal as comapared to the narrower potential scan in **Figure 1B** (i.e. the oxidation peak current in **Figure 1B** was 381 μA, higher than the value of 297 μA in **Figure 1A**). Thus, in real-time sensing, the potential region wherein only oxidation of 2,4-TDI occurs is selected. The abovementioned experiments supported our rationale to study the optimal 2,4-TDI sensing conditions as well as demonstrating the benefit of employing IL in these sensor developments.

To further investigate the electrochemical process of 2,4-TDI and to mimic real-world sensing conditions, similar cyclic voltammetric experiments were conducted using air as the background gas, as shown in **Figure 2**. Oxygen is ubiquitous in the ambient environment and plays significant roles in any sensing method development. Especially because its presence can also modify electrochemical processes in ILs, even though the reductively generated superoxide anion radical is more stable than in other solvents. Xiao et al. have reported the effect of the superoxide radical on carbon dioxide electrochemistry.[33] Herein, it

is shown that for a narrow potential scan wherein oxygen reduction processes are not involved, a clear and large 2,4-TDI oxidation peak was observed (red curve). The same was true for the experiment with a wider potential window, but with initiating the scan in the anodic direction, thereby performing the 2,4-TDI oxidation before its reduction (green curve). However, when the scan direction was first in the cathodic potential, involving the generation of superoxide shown by a reduction peak at ~−1.4 V, the peak for the oxidation of 2,4-TDI almost disappeared (see the blue curve). From this data, two important conclusions can be drawn. First, 2,4-TDI can react with the reduction products of the most important environmental interferent, oxygen,[40] thereby leaving no TDI at the interface to be detected. This property can be used for removing toxic TDI. But, it supports the choice of using only the oxidation processes for quantification, as shown by the results of these experiments, especially if the electrochemical 2,4-TDI sensor has to be used in real ambient environments. Second, this experiment also shows the selectivity of the sensing system for 2,4-TDI under the chosen experimental conditions. The peak at 1.38 V is clearly due to the presence of 2,4-TDI, which remains there in the presence of oxygen and all other air gases, although it disappears in the presence of superoxide due to their reaction. Thus, if the fomation of superoxide radical is avoided by choosing a specific potential window, 2,4-TDI can be selectively detected in real ambient environments.

For further elaboration of the electrochemical reaction mechanisms for the abovementioned processes, we performed the CV at various scan rates. **Figure 3** shows the cyclic voltammogram of 0.1% v/v 2,4-TDI in [C_4mpy][NTf_2] at scan rates of 10 mV/s – 500 mV/s. An oxidation peak potential shift (from 1.77 V to 1.24 V) was observed when the scan rate was changed from 500 mV/s to 10 mV/s. For a fast, electrochemically reversible system, the peak potential does not shift at different scan rates. In the case of 2,4-TDI, the electrode reaction is an irreversible process even at a slow scan rate (e.g. 10 mV/s). Thus, the peak potential shift is suggested to be the results of multiple coupled reactions, e.g. chemical reactions coupled with the electrochemical reactions or the electron transfer reaction reactions rather than the uncompensated IR drop, based on the following results: (1) the peak current has a linear relationship with the scan rate, supporting a surface controlled electron transfer process; (2) the increase of impedance vs. frequency in EIS measurement at various time intervals (**Figure 5**) supporting the surface reactions discussed below.

Furthermore, it is important to note in **Figure 3** that a shoulder peak started to emerge at about 0.8 V. This is more evident at faster scan rates. Kuroiwa et al.[41] have reported a similar shoulder peak for the oxidation reaction of chlorophyll a in IL/acetonitrile mixture, whereas this peak can be de-convoluted from the voltammogram and the resulting peak current can be estimated by using Gaussian curve fitting methods. The peak current ratio of P_I/P_{II} decreases as the scan rate increases (from 0.251 at 10 mV/s to 0.0254 at 500 mV/s) where P_I is the shoulder peak and P_{II} is the main oxidation peak, which suggests that the first oxidation process (P_I) has relatively slower kinetics and can be related to the aggregation of the analyte molecules as was the case with chlorophyll a. Furthermore, the sufficiently large oxidation current for this peak strongly supports the idea that analyte molecules form a low-order aggregate, such as a dimer, because high-order aggregates would not yield sizeable oxidation currents due to slow diffusion. Such aggregation

processes have been reported to lower the oxidation potential of the analyte in addition to the similar effects caused by IL ion-pairing. To further investigate this peak P_I and to validate the possibility of a dimerization process, a series of CV measurements with different time intervals were designed. In this experiment, 2,4-TDI was equilibrated in the IL electrolytes at different times and then the measurements were performed. The 2,4-TDI oxidation peak current decreased when the CV measurements were performed at longer time intervals (**Figure 4A**). No peak shift was observed as was the case during the variation of scan rates. The peak current values followed a first-order exponential decrease (**Figure 4B**) with a correlation coefficient equal to 0.994. This exponential decay of the 2,4-TDI oxidation peak current can also be utilized for a selectivity study of the future sensor device. In **Figure 4A**, the shoulder oxidation peak (P_I, located at 0.8 V) was also observed. This peak was more clear at longer time intervals (e.g. 1000 min) and fairly insignificant when the measurement was carried out instantaneously (0 min). The reduced current signals for P_{II} and increasing current signals for P_I with increasing time of measurement could only be attributed to the adsorption of 2,4-TDI at the electrode surface by the formation of dimers, trimers and even polymers, through isocyanate self-addition reactions (eq.1 & eq.2, where R is defined as the toluene aromatic ring), which lowered the concentration of electrochemically active species near the electrode surface.

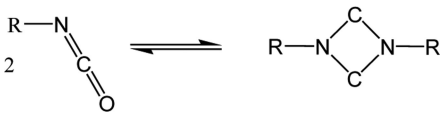

(eq. 1)

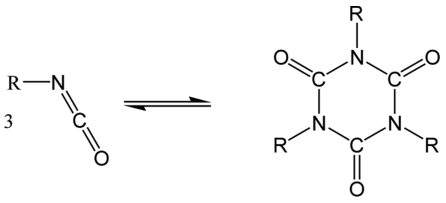

(eq. 2)

We performed electrochemical impedance analysis to understand further about the interface reactions at different time scales. EIS results can provide valuable information about the dynamic surface adsorption processes of 2,4-TDI in the [C_4mpy][NTf_2] electrolyte. EIS has been used to study many surface reactions such as dye and surfactant dimerization processes.[42] Thus, EIS experiments were carried out at several time intervals in the presence of 2,4-TDI at an open circuit potential. As shown in **Figure 5A and Figure S3**, the Nyquist plots change at various measurement times. As shown in **Figure S3**, we simulated the EIS curves by carefully selecting the equivalent circuit according to the literature. Among all the equivalent circuit models we employed to fit the experimental data, the one that obtained the best fit is presented in the inset of **Figure S3**. These simulated results are not good fits, especially at the zero hour. We believe that the deviation from a perfect fit is an indication

for the dynamic chemical reactions (i.e. the TDI self-polymerizations). **Figure 5B**, the Bode curves of the EIS experiment present the correlation of log |Z| versus log frequency at different time intervals. The Z' versus frequency and Z" versus frequency plots (**Figure S3 C-D**) show that the real part of the impedance increases with time at low frequencies much more than the imaginary part of the impedance. It is clear that the surface reactions cause the impedance to increase at longer time intervals, especially at low frequencies. Such trends can also be observed in the Nyquist plots too (**Figure 5A**) and are similar to the ones reported earlier for different surfactants and dyes in dimerization/aggregation reactions.

Results from the EIS experiments confirm the presence of dynamic interface processes of 2,4-TDI and are consistent with the results presented in **Figure 4**. Toluene was used as a negative control to further understand the 2,4-TDI oxidation processes in the IL at the glassy carbon electrode. The selection of toluene as a reference sample was due to its similar chemical structure as 2,4-TDI except the two isocyanate groups (–N=C=O). No oxidation peak was observed in the toluene sample with the same conditions as for 2,4-TDI. Thus, the oxidation peak and the consequent surface modification/dimerization are attributed to the isocyanate groups.

Identifications of Interface Products by UV-vis and FT-IR—UV-Vis and FT-IR spectroscopy experiments were employed to determine the 2,4-TDI oxidation products for additional insights on the reaction mechanism. There are two possible molecular sites for 2,4-TDI oxidation: 1) the C-N single bond cleavage at the 2 and/or 4 position of the benzene ring or 2) the N=C double bond cleavage in the isocyanate functional group. First, UV-Vis measurements (**Figure 6A**) were performed to characterize samples of different 2,4-TDI concentrations in $[C_4mpy][NTf_2]$ as well as the sample of pure $[C_4mpy][NTf_2]$ as the background. As the concentration of 2,4-TDI increased, the absorbance peak at 290-300 nm[43] also increased with a red shift, indicating an enhanced delocalized conjugation effect. This could be attributed to isocyanate self-addition forming isocyanate polymers. We also characterized the bulk IL near the glassy carbon electrode surface after an electrochemical oxidation of 2,4-TDI was conducted. A significant decrease of the absorbance and a blue shift were observed from this bulk IL sample. The absorbance peak changes indicated that there was a reduced conjugation of the 2,4-TDI molecular structure, which could be attributed to the loss of the isocyanate functional group due to electrochemical oxidation of 2,4-TDI, causing a decrease of the delocalized conjugation effect.

FT-IR measurements (**Figure 6B**) were carried out to obtain additional information in terms of identifying the bond breaking of the isocyanate functional group. An absorbance peak at 2279 cm^{-1} was observed from $[C_4mpy][NTf_2]$ in the presence of 0.5% v/v 2,4-TDI. This peak was not found in either pure $[C_4mpy][NTf_2]$ or the $[C_4mpy][NTf_2]$ sample that was taken from the bulk solution near the glassy carbon electrode surface after an electrochemical oxidation of 2,4-TDI was performed. According to Thomson et al.,[44] the absorbance peak at 2279 cm^{-1} could be assigned to the asymmetric vibration of N=C=O functional group. This illustrated that the NCO functional group disappeared. Thus, it is plausible that the N=C double bond was cleaved during 2,4-TDI oxidation. Thus, the plausible mechanism is an CECE mechanism depicted as follows (R is defined as the

toluene aromatic ring, we use the dimer as a case study), in which the chemical process is the rate limiting step:

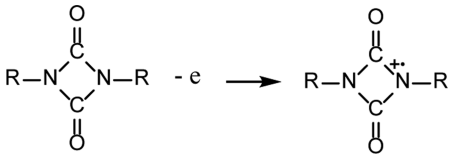

(eq. 4)

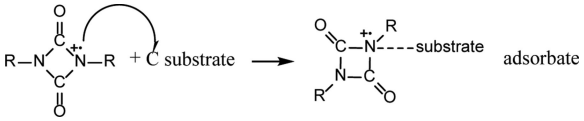

(eq. 5)

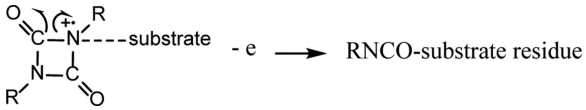

(eq. 6)

2,4-TDI monomer undergoes a self-addition reaction in the initial state (eq. 3). When an external anodic potential is applied, eq. 4 occurs yielding a stable radical product due to the delocalized electron conjugation effect. It is followed by a surface adsorption process (eq. 5, C stands for glassy carbon) at anodic conditions. This step is rate-limiting because of the reactivity of the carbon surface. Then, a second oxidation occurs involving the C-N bond breaking forming adsorbate residues (eq. 6). This proposed mechanism complies with CV data in **Figure 4A** that the shoulder peak becomes more significant at longer testing time intervals.

Sensing Characterization of TDI Oxidation in ILs

Once the mechanisms of electrochemical oxidation of 2,4-TDI had been understood using electrochemical, EIS, and spectroscopic techniques, we now had the guidelines to design electrochemical methods for evaluating the sensing performance utilizing those mechanisms. Usually, the sensor is first employed to do sensitivity tests by exposing it to different concentrations of the analyte. However, we first performed selectivity tests to clear out the following important points of this study. The selectivity experiments for the compounds similar to the molecule under study can provide an indirect proof of the dimerization process suggested for 2,4-TDI. Second, the presence of dimerization, if it is the case only with TDI, the detection/sensing mechanism can be made to be very selective, which is the most important requirement of present day sensors.

Selectivity experiments for 2,4-TDI—2,4-TDI was selected as the representative molecule of the isocyanates class, because it has a high vapor pressure of 0.05 mm Hg and is the most common airborne isocyanate. As described earlier, toluene can be used as a negative control for 2,4-TDI oxidation process as it has the same structure with the absence of isocyanate groups. However, it can also be tested as an interfering molecule for 2,4-TDI detection. When toluene was subjected to the electrochemical oxidation process, no oxidation peaks were observed, as shown in **Figure S1**, even for a concentration of 4%. In the same experiment, TDI at a much lower concentration showed reproducible signals. In the other experiment, aniline, which is quite well known as an oxidizable compound, was tested in comparison with 2,4-TDI. At the same concentration and under the same conditions, aniline showed an oxidation current even larger than the target (**Figure S2**), though the peak potential of aniline is quite different. Thus, different electrochemical techniques, such as chronoamperometry, can be used to selectively detect the target isocyanates by choosing a certain measurement potential.

However, the most important observation in this regard came from the time lapse experiment carried out with aniline and 2,4-TDI, the data is shown in **Figure 7**. As indicated, no significant change in the oxidation current signal occurs in the IL that contains aniline but the same shoulder peak is present in IL containing TDI, thereby decreasing the oxidation peak current with every time step. This indirectly proves the self-addition reaction of TDI, and alongside, this mechanism can serve to provide an extremely selective response mechanism for TDI detection with signal diminishing as a function of time. In addition, Yakabe et al.[45] reported that aniline and 2,4-TDI exhibit different side reactions in the presence of trace water (i.e. 2,4-TDI produces CO_2 when reacted with water), which can be utilized to enhance the selectivity of the detection.

Detection of 2,4-TDI in Liquid and Gas Phases—Finally, the sensitivity experiments were performed to evaluate LODs and T_{90} for the developed sensor mechanism. To perform liquid phase 2,4-TDI detection, 2,4-TDI was directly added into the electrochemical cell with $[C_4mpy][NTf_2]$ electrolyte in an air environment. The concentration of 2,4-TDI was varied from 0% v/v to 0.5% v/v, with 0.1% v/v increments. The cyclic voltammograms and the corresponding calibration curves are presented in **Figure 8**. The value of the correlation coefficient (R^2) was calculated to be 0.997. The detection sensitivity could be obtained from the slope of the linear fitting curve, which was 252.6 μA/μL. By analyzing the mean background signal (S_{bm}) and the corresponding standard deviation (s_{bm}) value, the minimum distinguishable signal (S) can be obtained via eq. 7. Thus, the limit of detection (LOD) can then be converted from S in the calibration equation shown in **Figure 8B**. LOD in this liquid phase 2,4-TDI sensor is 0.0651 μL in 500 μL, which equals to 130.2 ppm.

$$\mathrm{S}=\mathrm{S}_{bm}+3*^{S}bm \quad \text{(eq. 7)}$$

For gas sensing, one of the most important aspects is the sampling of analyte gases. The use of hydrophobic, non-volatile IL as an electrolyte enables a simple gas sampling system that can be open to the ambient environment. This not only allows pre-concentration to further

increase the sensitivity of the detection, but can also significantly simplify future sensor system integration and provide long sensor lifetimes. Real-time current response recording (**Figure S4**) in gas phase sensing was performed via chronoamperometry at different 2,4-TDI concentrations. **Figure 9A** presents the chronoamperometry data with time offsets by showing the sensor response when 2,4-TDI is added and by removing the non-Faradic current decay period. Becasue the 2,4-TDI sample is in liquid form, a sampling system consisting of two gas paths was designed and depicted in **Scheme S2**. By adjusting the flowrates of the two gas paths, an accurate amount of gas phase 2,4-TDI can be calculated (i.e. the gas phase 2,4-TDI is 32.89 ppm when the flowrate of both gas paths is 100 sccm). The external potential was set at 1.4 V, based on the cyclic voltammogram in **Figure 8**. Each measurement was carried out in samples that were separately prepared. Air was used as the background gas in order to fully explore the real life potential of the sensor. The sensing current reached a signal plateau at about the 600^{th} second. It is interesting to note that the sensing current curve exhibits two stages. This observation is consistent with the CV data presented in **Figure 3** and **Figure 4A**, indicating that there are multiple reactions involved.

The plot of sensitivity values at different sensing time scales (**Figure 9B**) also demonstates that there are two separate electrochemical steps, of which the transition point is the 200^{th} second. Detailed calibration curves at various sensing time scales are shown in **Figure S5**. By analyzing the sensor response at different time scales, properties such as sensitivity and LOD values vary (**Table S2**). For example, when picking the signal plateau at the 600^{th} second, the sensitivity is 1.942 μA/ppm with a value of LOD at 0.7693 ppm. However, if picking one of the times before the plateau (e.g. 100^{th} second), the sensitivity decreases to 0.2083 μA/ppm with a relative higher value of LOD (12.46 ppm). Moreover, T90 values of this sensor to function for 100 and 600 seconds are calculated to be 90.80 seconds and 432.3 seconds, respectively. Thus, by sacrificing the sensor response time, higher sensitivity and lower LOD values can be approached, which gives this sensor a potential to tune different functioning times for different sensing needs.

CONCLUSIONS

A new electrochemical detection method was established for 2,4-TDI detection directly in the liquid phase, as well as the gas phase. This sensing methodology was based on the use of non-aqueous non-volatile IL $[C_4mpy][NTf_2]$, which provided stable and reliable detection conditions. In addition, the strong ion-pairing in ILs can play a role in modifying the electrochemical process in such a way that it can facilitate the design of sensors, as in this case. The oxidation of 2,4-TDI is a single step process in ILs with lowered oxidation potentials.

The detection of 2,4-TDI utilizing the oxidation process, because it has an electron-abundant molecular structure that is prone to lose electrons and be oxidized, was accomplished under a set of optimal reaction conditions that were defined as a result of detailed electrochemical studies. 2,4-TDI reactions were discussed in terms of reaction dynamics and the electrolyte-electrode interface. By utilizing ILs as the electrolyte, the sensor can respond at a relatively lower potential than other common solvents (e.g. acetonitrile). Molecules of 2,4-TDI were found to self-accumulate and undergo inter-molecular dimerization via self-addition,

suggesting a surface modification when the TDI is measured at various time scales, and the potential to enhance selectivity. Spectroscopic methods were able to identify the occurrence of 2,4-TDI self-addition reactions and that the 2,4-TDI oxidation occurred at the isocyanate functional group. The selectivity experiments also provided an indirect proof of dimerization. Finally, liquid and gas phase detection was performed with the obtained detection limits capable of meeting the NIOSH regulatory number (2.53 ppm). In gas phase sensing, the sensitivity depends on the sensing time of this sensor, with higher sensitivity at longer sensor functioning periods. The use of a Clark-type electrochemical cell design[35] for this gas phase 2,4-TDI sensor allows the sensor to respond in a quicker time frame, because it shortens the gas molecule diffusion process in the IL. The use of a low cost carbon electrode material and non-volatile IL electrolyte makes this a promising low cost, miniaturizable and disposal sensor. Electrochemical detection based on the oxidation of the isocyanate functional group provides good selectivity and there is very little water present in the hydrophobic ILs used in this study. Thus, very little isocyanates can be lost due to chemical reactions that occur in conventional solvents such as water, alcohol, acids and organic solvents that contain primary or secondary amines. This benefit makes it much more powerful and lower cost detection technology. Thus, this simple electrochemical detection could be considered as a robust sensing method for practical detection of 2,4-TDI and might also be applicable for the detection of other isocyanate compounds.

Supplementary Material

Refer to Web version on PubMed Central for supplementary material.

Acknowledgement

X. Zeng likes to thank support of NIH R01 and Oakland University. The authors appreciate the constructive discussion with Dr. Zhe Wang, former postdoc and currently assistant professor at Xavier Univ. Louisiana for experiment design.

REFERENCES

1. Li J, Tian B. Science Bulletin. 2015; 60:1868–1870.
2. Guglya EB. J Anal Chem. 2000; 55:508–529.
3. Pronk A, Tielemans E, Skarping G, Bobeldijk I, Heederik VANHJ,D, Preller L. The Annals of occupational hygiene. 2006; 50:1–14. [PubMed: 16126758]
4. Henriks-Eckerman M-L, Valimaa J, Rosenberg C, Peltonen K, Engstrom K. Journal of Environmental Monitoring. 2002; 4:717–721. [PubMed: 12400920]
5. U.S. Department of Health and Human Services. Hazardous Substances Data Bank (HSDB, online database). National Toxicology Information Program, National Library of Medicine; Bethesda, MD.: 1993.
6. U.S. Environmental Protection Agency. EPA Chemical Profile on Toluene 2,4-Diisocyanate. 1987
7. Baether, W., Zimmermann, S., Gunzer, F. Sensors Journal. Vol. 12. IEEE; 2012. p. 1748-1754.
8. Tsai CJ, Lin HC, Shih TS, Chang KC, Hung IF, Deshpande CG. Journal of hazardous materials. 2006; 137:1395–1401. [PubMed: 16730902]
9. Ferreira HE, Condeco JAD, Fernandes IO, Duarte DE, Bordado JCM. Analytical Methods. 2014; 6:9242–9257.
10. Skarping G, Renman L, Sangö C, Mathiasson L, Dalene M. Journal of Chromatography A. 1985; 346:191–204.

11. Skarping G, Dalene M, Lind P. Journal of chromatography. A. 1994; 663:199–210. [PubMed: 8173666]
12. Zhu Y, Wang M, Du H, Wang F, Mou S, Haddad PR. Journal of Chromatography A. 2002; 956:215–220. [PubMed: 12108653]
13. Chen ML, Fan YC, Li CA, Fei D, Zhu Y. Chinese Chemical Letters. 2009; 20:207–209.
14. Schaeffer JW, Sargent LM, Sandfort DR, Brazile WJ. Journal of Occupational and Environmental Hygiene. 2013; 10:213–221. [PubMed: 23442121]
15. Kubitz KA. Analytical Chemistry. 1957; 29:814–816.
16. Lord SS. Analytical Chemistry. 1957; 29:497–499.
17. Lemons AR, Bledsoe TA, Siegel PD, Beezhold DH, Green BJ. Journal of Immunological Methods. 2013; 397:66–70. [PubMed: 24012971]
18. Morrison RC, Guilbault GG. Analytical Chemistry. 1985; 57:2342–2344.
19. Tang YA, Edelmann RE, Zou SZ. Nanoscale. 2014; 6:5630–5633. [PubMed: 24752282]
20. Yang HZ, Tang YG, Zou SZ. Electrochemistry Communications. 2014; 38:134–137.
21. Zhang L, Zhang Q, Li J. Journal of Electroanalytical Chemistry. 2007; 603:243–248.
22. Liu J, Morris MD, Macazo FC, Schoukroun-Barnes LR, White RJ. Journal of the Electrochemical Society. 2014; 161:H301–H313.
23. Liu J, Wagan S, Morris MD, Taylor J, White RJ. Analytical Chemistry. 2014; 86:11417–11424. [PubMed: 25337781]
24. Rehman A, Zeng XQ. Accounts Chem. Res. 2012; 45:1667–1677.
25. Liu HT, Liu Y, Li JH. Physical Chemistry Chemical Physics. 2010; 12:1685–1697. [PubMed: 20145833]
26. Mu XY, Wang Z, Zeng XQ, Mason AJ. IEEE Sens. J. 2013; 13:3976–3981.
27. Xia ZG, Wang JH, Hou YB, Lu QY. Review of Scientific Instruments. 2014:85.
28. Wang Z, Lin PL, Baker GA, Stetter J, Zeng XQ. Analytical Chemistry. 2011; 83:7066–7073. [PubMed: 21848335]
29. Wang Z, Mu XY, Guo M, Huang Y, Mason AJ, Zeng XQ. J. Electrochem. Soc. 2013; 160:B83–B89.
30. Xiao CH, Rehman A, Zeng XQ. Analytical Chemistry. 2012; 84:1416–1424. [PubMed: 22224654]
31. Xiao C, Rehman A, Zeng X. RSC Advances. 2015; 5:31826–31836.
32. Wang Z, Zeng XQ. J. Electrochem. Soc. 2013; 160:H604–H611.
33. Xiao CH, Zeng XQ. Journal of the Electrochemical Society. 2013; 160:H749–H756.
34. Relative reactivity of isocyanates with active hydrogen compounds. http://www.poliuretanos.com.br/Ingles/Chapter1/131Isocyanates.htm
35. New Jersey Department of Health and Senior Services. Hazardous Substance Fact Sheet".
36. Rehman A, Hamilton A, Chung A, Baker GA, Wang Z, Zeng XQ. Analytical Chemistry. 2011; 83:7823–7833. [PubMed: 21863884]
37. Atifi A, Ryan MD. Analytical Chemistry. 2014; 86:6617–6625. [PubMed: 24884098]
38. Fry AJ. Electrochemistry Communications. 2005; 7:602–606.
39. Wang Z, Guo M, Baker GA, Stetter JR, Lin L, Mason AJ, Zeng XQ. Analyst. 2014; 139:5140–5147. [PubMed: 25093213]
40. Sawyer DT, Valentine JS. Accounts of Chemical Research. 1981; 14:393–400.
41. Kuroiwa Y, Kato Y, Watanabe T. Journal of Photochemistry and Photobiology A: Chemistry. 2009; 202:191–195.
42. de Oliveira HP, de Melo CP. Journal of Physical Chemistry B. 2011; 115:6903–6908.
43. https://www2.chemistry.msu.edu/faculty/reusch/VirtTxtJml/Spectrpy/UV-Vis/spectrum.htm
44. Thomson MA, Melling PJ, Slepski AM. Abstracts of Papers of the American Chemical Society. 2001; 221:U316–U316.
45. Yakabe Y, Henderson KM, Thompson WC, Pemberton D, Tury B, Bailey RE. Environmental Science & Technology. 1999; 33:2579–2583.

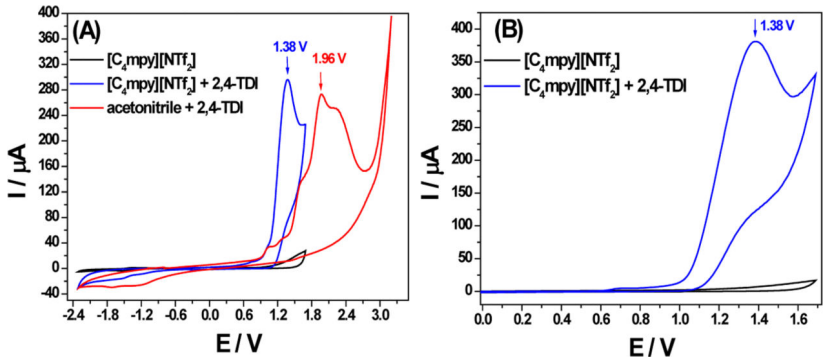

Figure 1.

(A) CV of pure [C_4mpy][NTf_2] (black), 1% v/v 2,4-TDI [C_4mpy][NTf_2] (blue), and 1% v/v 2,4-TDI in acetonitrile with 0.1 M TBAP as a supporting electrolyte (red). The concentration was 1.0% v/v. Glassy carbon, silver and platinum electrodes were used as the working, reference and counter electrodes, respectively. The scan rate was 100 mV/s. All potentials were calibrated based on the Fc/Fc^+ redox couple. N_2 was used as the background gas. CV scanned toward the negative potential direction first. (B) CV for 1 mL of pure [C_4mpy][NTf_2] and in the presence of 1% v/v 2,4-TDI in the potential window of 0 to 1.7 V. All curves presented here are taken from the first cycle of the CV measurements.

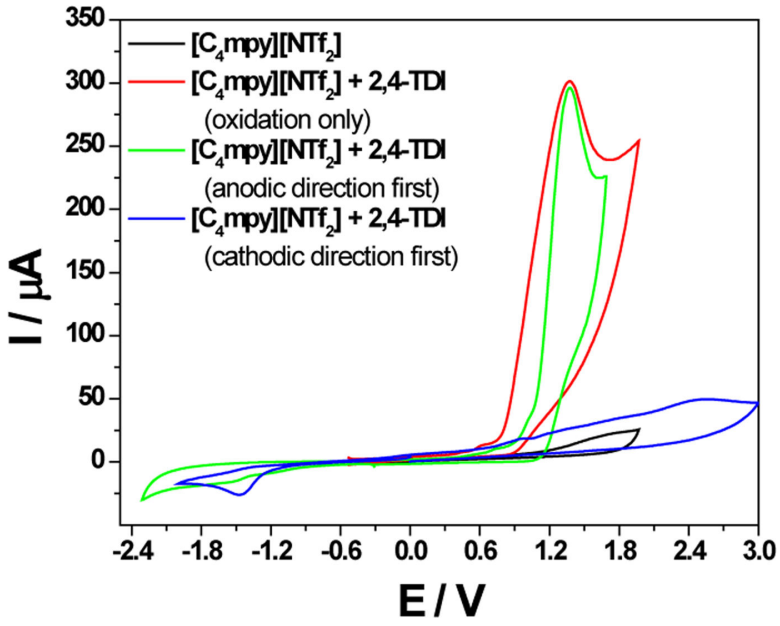

Figure 2.

CV of pure $[C_4mpy][NTf_2]$ (black), in the presence of 1.0% v/v 2,4-TDI in the narrow anodic potential window (red), in wider potential window scanning to the anodic potential direction first (green), and in wider potential window scanning to the cathodic potential direction first to form superoxide radical thereby showing no oxidation current for 2,4-TDI (blue). Air was the background gas for all these measurements. All curves presented herein are taken from the first cycle of the CV measurements.

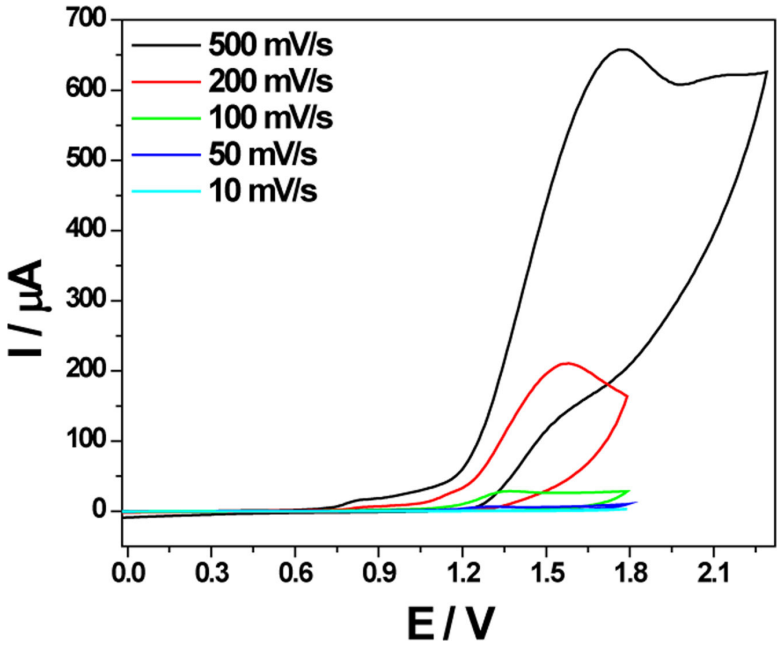

Figure 3.

CV of 0.1% v/v 2,4-TDI in [C_4mpy][NTf_2] with varying of scan rates. Glassy carbon, silver and platinum electrodes were used as the working, reference and counter electrodes, respectively. All potentials were calibrated based on the Fc/Fc^+ redox couple. Air was the background gas for all these measurements. All curves presented herein are taken from the first cycle of the CV measurements.

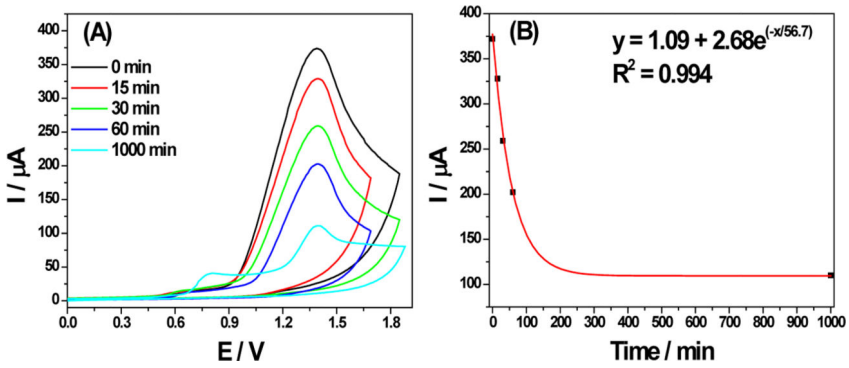

Figure 4.

(A) CV of 2,4-TDI oxidation process in [C_4mpy][NTf_2] in an air environment, on a glassy carbon electrode. The concentration of 2,4-TDI was 10 μL in 1 mL ionic liquid (1.0% v/v). Silver and platinum wires were the reference and counter electrodes, respectively. Measurements were performed with different time intervals after the three-electrode system had been setup. The scan rate was 100 mV/s. All potentials were calibrated based on the Fc/Fc^+ redox couple. All curves presented herein are taken from the first cycle of CV measurements. (B) The corresponding calibration curve. Air was the background gas for all these measurements.

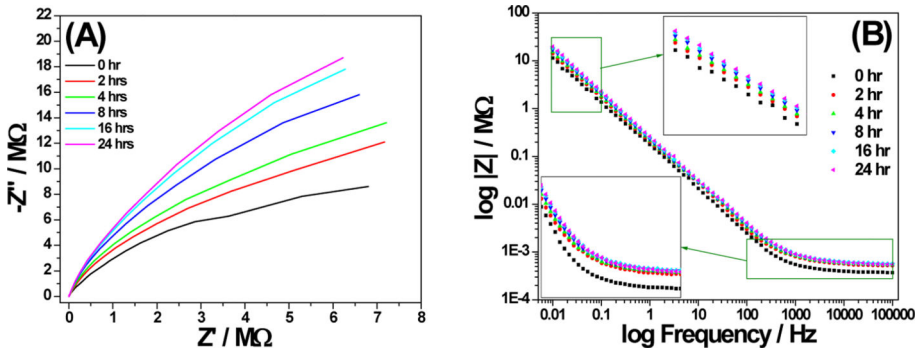

Figure 5.

(A) Nyquist plots measured at various time intervals with 1% v/v 2,4-TDI in $[C_4mpy][NTf_2]$ on a glassy carbon electrode. Silver wire and platinum wire were the reference and counter electrodes, respectively. (B) The Bode plots measured at various time intervals with 1% v/v 2,4-TDI in $[C_4mpy][NTf_2]$ on a glassy carbon electrode. Silver wire and platinum wire were the reference and counter electrodes, respectively. (C) The Bode plots of Z' (the real part of the impedance) changes at different frequencies. (D) The Bode plots of Z" (the imaginary part of the impedance) changes at different frequencies. The EIS experimental parameters: AC bias was 5 mV, and the DC input was 0 V vs. open circuit. Air is the background gas.

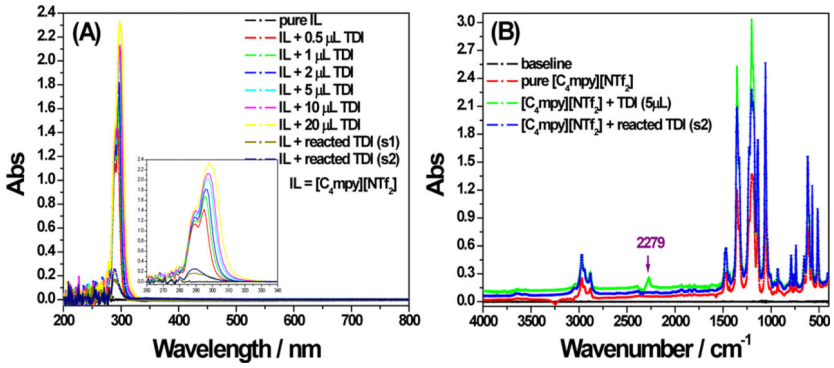

Figure 6.

Spectroscopic characterization of the electrochemical reaction of 2,4-TDI in $[C_4mpy][NTf_2]$ on the glassy carbon surface: (A) UV-Vis method, and (B) FTIR method (transmission mode). 2,4-TDI concentration varied from 0.05% v/v to 2% v/v.

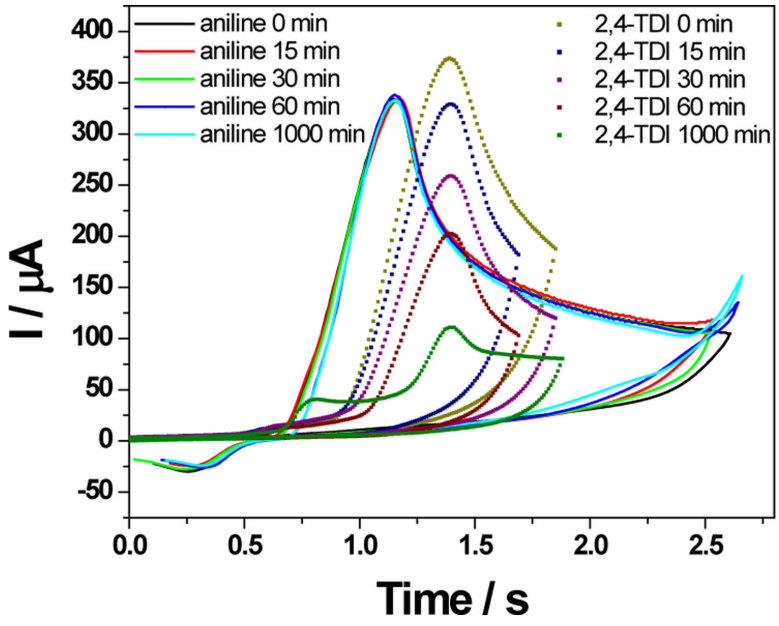

Figure 7.

CV of $[C_4mpy][NTf_2]$ adding 1% v/v aniline (solid lines) and 1% v/v 2,4-TDI (dotted lines), at different testing time intervals, in air. Glassy carbon, silver and platinum electrodes were used as the working, reference and counter electrodes, respectively. Measurements were performed with different time intervals after the three-electrode system had been setup. The scan rate was 100 mV/s. All potentials were calibrated based on the Fc/Fc^+ redox couple. All curves presented here are taken from the first cycle of the CV measurements.

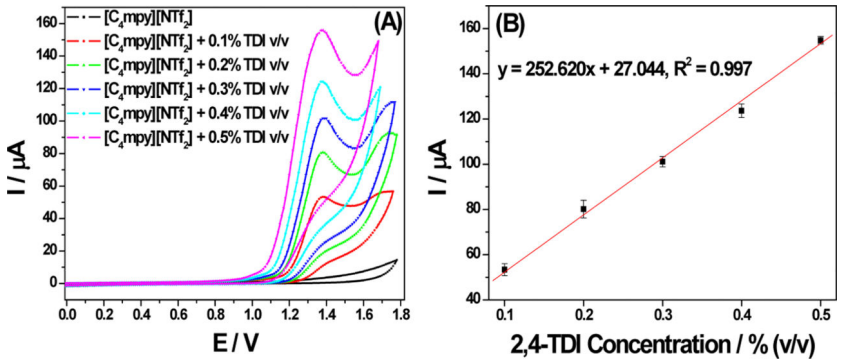

Figure 8.

(A) CV sensing of liquid phase 2,4-TDI in $[C_4mpy][NTf_2]$ on a glassy carbon electrode, in air. Concentration of 2,4-TDI varied from 0.1% v/v to 0.5% v/v. Silver and platinum electrodes were used as the reference and counter electrodes, respectively. The scan rate was 100 mV/s. All potentials were calibrated based on the Fc/Fc^+ redox couple. All curves presented here are taken from the first cycle of the CV measurements. (B) Calibration curve of the current vs. 2,4-TDI concentration, with error bars. Air is the background gas.

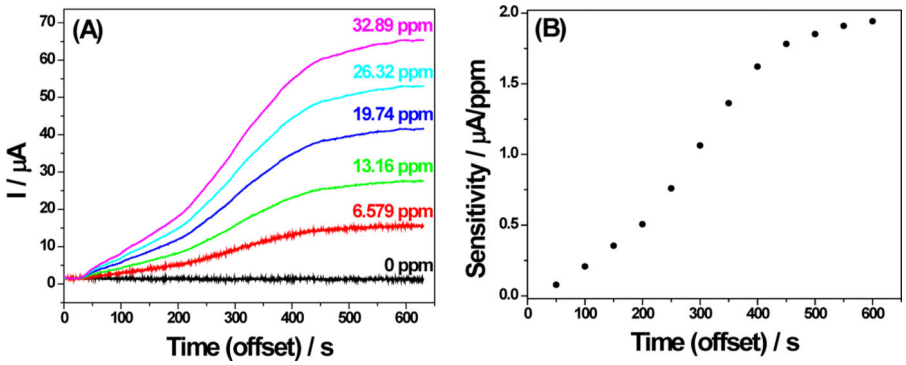

Figure 9.

(A) Real time chronoamperometry detection of gas phase 2,4-TDI in [C_4mpy][NTf_2]. External potential was set constant at 1.4 V. Glassy carbon, silver and platinum electrodes were used as the working, reference and counter electrodes, respectively. Air was the background gas. Data sampling rate is 0.2 second per data point. (B) Plot of the selected sensitivity values at different time scales.